Nuclear Materials Authority
P.O.Box 530 Maadi, Cairo, Egypt

ISSN 2314-5609
Nuclear Sciences Scientific Journal
13, 48-68
2024
https://nssi.journals.ekb.eg

THE LITHOLOGICAL AND STRUCTURAL FEATURES CONTROLLING THE RADIOACTIVE MINERALIZATIONS IN YOUNGER GRANITES OF WADI BALI AND WADI UMM SIDRAH AREA, NORTH EASTERN DESERT, EGYPT

Abd El Naby, A. S.[2], El Mezayen, A. M.[1], El Kholy, D. M.[2] and Khames, H. A.[2]
1. Geology Department, Faculty of Science, Al Azhar University, Egypt.
2. Nuclear Materials Authority, P.O. Box 530, Maadi, Cairo, Egypt.

ABSTRACT

The study area is located in the northern part of the Eastern Desert of Egypt. It is situated in the northern sector of Red Sea mountain ridges at about 65 km northwest of Hurghada City and is considered as one of high potentialities for uranium deposits. The study area comprises the younger granite of Gabal (G) Gattar, Hammamat sedimentary rocks of Gabal (G) Umm Tawat, Dokhan volcanic rocks in the centeral part of the area which are contacted northward by the younger granites of Gabal (G) Abu Harba. The younger granites are the most common rock type in the study area. There are two types of these granites: Gattar alkali feldspar granite to syenogranites and Abu Harba syenogranites.

The structural deformations of the study area are represented by primary structures and secondary ones. The most prevailing structures are folding, faulting and jointing. The main trends of faults are NNE-SSW, NNW -SSE, N-S, NW-SE, NE-SW and WNW-ESE trends. All of these faults are of compression stress. The faults, especially those trending in the NNE-SSW and N-S are the main passways to the ascending uranium-bearing hydrothermal solutions. The study area is also affected by five main sets of joints trending NNE-SSW, N-S, NE-SW, WNW-ESE and NW-SE. All joints in the area are of tension stress.

The gamma-activity measurements of the study area lead to the discovery of several occurrences. These occurrences are studied geologically, structurally and radiometrically in detail. The uranium content of the mineralized samples range from 155 ppm to 5570 ppm. The younger granites show higher radioactivity than that of the other rock types. It contains U and Th bearing minerals such as uranophane, thorite and zircon in addition to apatite, sphene and iron oxides which capture U and/or Th elements. Along GII occurrence the eU ranges from 59 to 4810 ppm with average 1271 ppm, while Th contents ranges from 13 to 270 ppm with an average 64ppm. At GV occurrence the eU ranges from 15 to 2740 ppm with an average 588, while Th contents range from 12 to 470 ppm with an average 90 ppm.

Keywords: Younger Granites, Wadi Bali, Wadi Umm Sidrah, Younger Granite, Gabal Gattar

INTRODUCTION

The study area is located between latitudes 27º 06′ 35″ - 27º 15′ 40″ N and longitudes 33º 14′ 11″ - 33º 20′ 61″ E in the northern part of the Eastern Desert of Egypt (Fig .1a)

Stern (1985) concluded that the NED is dominated by NE-SW structural trend. Hamimi et al. (2019) stated that the shear zones are the most prominent tectonic features in the Eastern Desert playing a major role in the structural shaping of the Neoproterozoic Pan-African belt. He also noted that the NED is dominated by fault/joint systems and marked by younger granitoid intrusions.

Many radioactive mineralizations are found in NED as in younger granites of Wadi (W) Hammad area (Khamis, 1995), Gabal (G) Abu Harba granitic batholith (Roz, 2001; Abdel Hamid, 2013).

The radioactive mineralizations in NED are controlled by geological and structural features. Shear and fault zones of NNE-SSW directions are associated with secondary uranium mineralization at G. Gattar (Roz, 1994). The uranium mineralization are located along a footwall of shear zone striking ENE-WSW to NE-SW direction at W. Bali area (Salman, et al, 1990 & Waheeb and El Sundoly, 2016). The NNE-SSW to NE-SW and NW-SE shear zones are responsible for the localization of uranium minerals in G-II uranium occurrence at G. Gattar (Waheeb, 2017). The uranium content of the G. Gattar granite area is with an average of 11.3ppm (Waheeb, 2022) suggesting a fertile-U source. The uranium occurrence at G.Abu Harba area is recorded along a mylonitic normal fault zone or shear zone trending N15ºW with dips of about 86º to SW. The gamma radioactivity measured over this anomaly reaches 1800 ppm (Waheeb and Samaan, 2021).

The aim of this research is to study the different rock types covering the study area and the structural elements affecting them. Also studying the role of the structures controlling the radioactive mineralizations in younger granites along Wadi Bali and Wadi Umm Sidrah area, North Eastern Desert, Egypt.

GEOLOGICAL SETTING

Based on the field studies, the main rock types exposed in the study area can be chronologically arranged from oldest to youngest as: Dokhan volcanics, Hammamat sedimentary rocks, younger granites and post granite dykes. A detailed geologic map (scale

1:40,000) for the study area is constructed (Fig. 1b).

Dokhan volcanics are widely distributed in the northern part of the study area. They are moderately to highly relief, massive, fine to very fine grained and range in color from pink, brownish red and red colors in the more acidic varieties, while the intermediate ones are gray to dark gray or green. They are represented by acidic (dacites, rhyodacites and rhyolites) and intermediate (andesites) lava flows with their associated pyroclastics of (tuffs and agglomerates). They are cut by different types of faults that cause a very distinctive rugged topography. They are highly jointed showing well developed columnar joints (Fig. 2a).

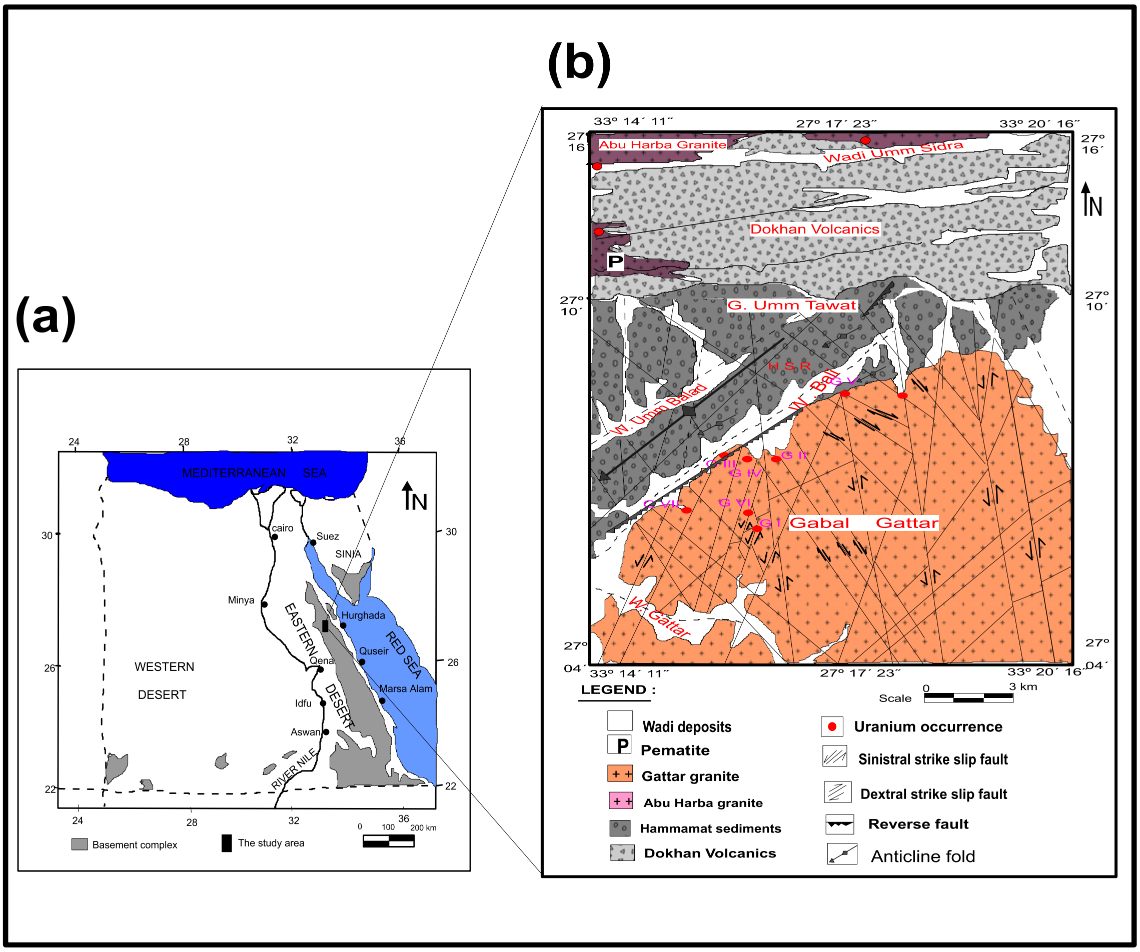

Fig. 1: (a) Location map of the study area, North Eastern Desert, (b) Geologicaland structure map of the area between W. Bali and W. Umm Sidrah).

Hammamat sediments are the most predominant rocks in the study area and occupy the central part of the mapped area (Fig.1b). These rocks crop out as relatively low hill masses, filling the inter-mountainous basin that separate the Dokhan volcanics from Gabal Gattar granite. They are separated from the granite by an ENE-striking dip slip reverse fault extending about 2.5 km along W. Bali (Shalaby 1990). These sediments are green, grayish green to dark gray in color, foliated, and well jointed. Unlike the type locality at W. Hammamat, the Um Tawat Hammamat sediments do not contain hematite-rich varieties (Dardir and Abu Zeid 1972). They consist of conglomerate, sandstone greywacke, siltstone, and mudstone.

The younger granites represent the main rock type in the investigated area. There are two types of these granites: Gattar alkali feldspar granite to syenogranites and Abu Harba syenogranites.

Gabal Gattar granites represent the northern part of a large batholith of younger granites. The age of these granites is about 575 Ma (Stem & Hedge 1985). The contact between the granites and the Hammamat sediments is sharp intrusive contact with slight metamorphism in these sediments (Fig. 2b). Gabal Gattar granites are predominantly formed of medium grained rocks varying in color from pink to reddish pink in fresh samples and pale pink to reddish brown due to alteration along shear zones. The commonest alterations in these granites are hematitization, silicification, episyenitization, fluoritization, kaolinitization and epidotization besides the frequent presence of manganese dendrites and carbonates.

Gabal Abu Harba granites covering an area of about 40Km^2. In these parts, the syenogranite is commonly of high rough topography with serrated peaks and smooth slopes. They are cut by faults and fractures that cause a very distinctive shearing and alterations of these granites. These granites intruded the Dokhan volcanics at its eastern and southern boundaries with sharp intrusive contacts (Fig. 2c). The northwestern outcrops of the syenogranite form a low to moderate relief when compared to other exposures of the same rock. They are coarse-grained and porphyritic with pinkish white color but turn to brownish red when stained with hematite along joint and fracture planes. It is characterized by scarcity of xenoliths, if present; they are mainly of ellipsoidal shape with either angular or curved edges (Fig. 2d). The most common alteration features are, hematitization, silicification, chloritization and epidotization as well as dendritic manganese oxides.

Post granite dykes are represented by acidic, intermediate and basalt. Gabal Gattar is younger than the intermediate and acidic dykes that not pass through it but stopped at its body, while basalt dykes cut G. Gattar. Gabal Abu Harba is cut by all dyke types. These dykes are varying in thickness from 0.5 m to10 m and extend for several kilometers in length. They run parallel to each other in swarms striking from NE-SW to ENE-WSW.

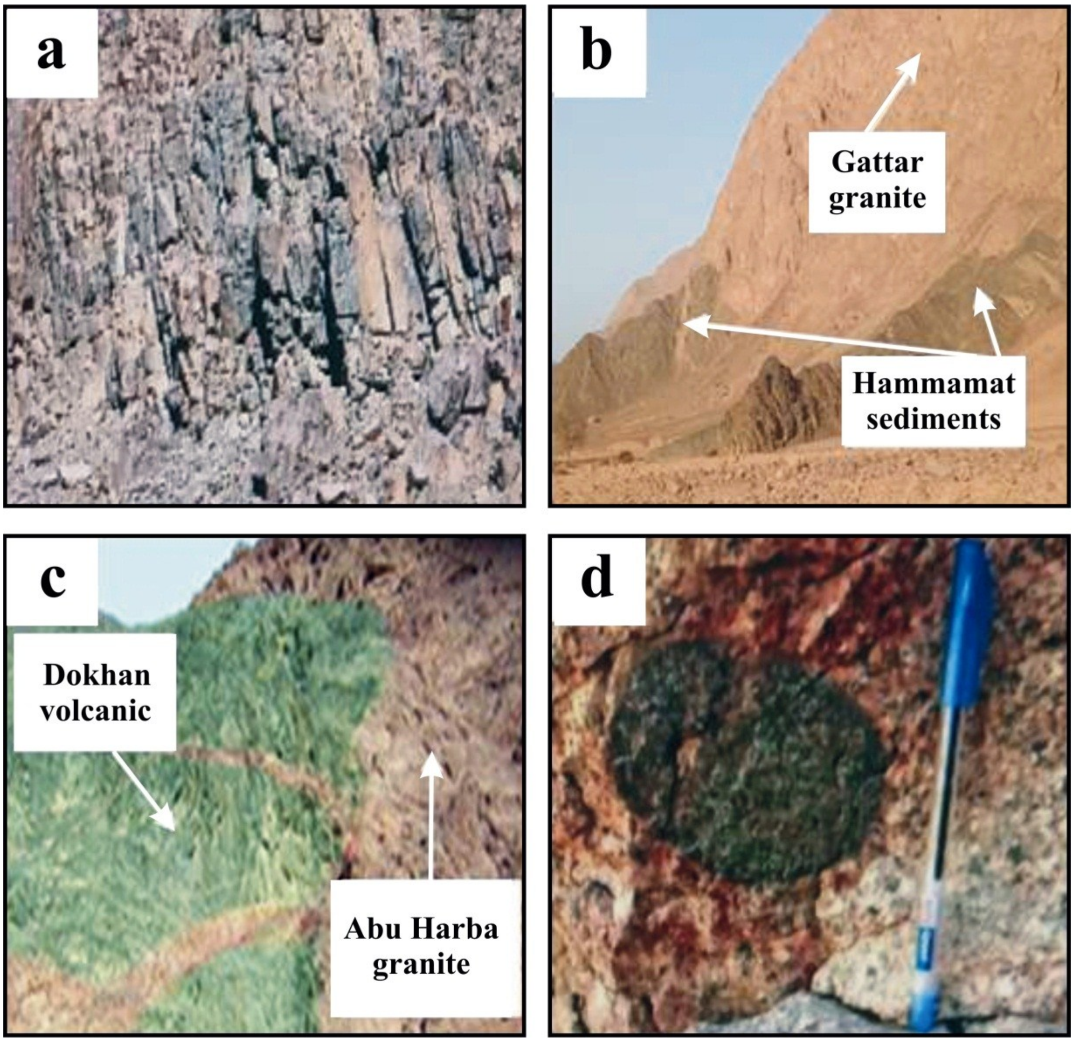

Fig. 2: Field photographs show (a) Well-developed columnar joints in Dokhan volcanics along W. Umm Sidra, looking NW, (b) Irregular Intrusive contact between G. Gattar younger granites and Hammamat sedimentary rocks along W. Bali, looking E, (c) Sharp contact between Abu Harba younger granite and Dokhan volcanic along W. Umm Sidra, Looking S. (d) Small mafic xenolith of Dokhan volcanic in younger granite, G. Abu Harba along Wadi Umm Sidrah ; Looking NE.

STRUCTURAL SETTING

The study area is characterized by some primary and secondary structures developed in the igneous and sedimentary rocks. The primary structures include bedding, graded bedding, cross bedding and ripple marks in Hammamat sedimentary rocks, flow and vesicular structures in Dokhan volcanics while the secondary structural elements are foliation, pencil structures, folds, faults and joints.

Bedding is the main primary structure which characterizes the Hammamat sediments. It is the planes that separate between the different Hammamat sedimentary rocks. Bedding is easily distinguished by the differences in color, texture, composition, and resistance to erosion. The Hammamat sediments show very clear bedding in all rock units including conglomerates, sandstone, siltstone, and mudstone (Fig. 3a). Generally, bedding strikes toward

NE-SW and dipping 15˚ to 25˚ SE. At the contact between G. Um Tawat and G. Dokhan, bedding is dipping gently at 25° toward N-W. In the other side, near G. Gattar, bedding dips steeply toward SE at about 70° or more along W. Mayyit Al-Abd and W. Bali at the contact with G. Gattar, indicating that the contact is affected by fault.

Foliations are observed in the siltstones and mudstones of the Hammamat sediments. Foliations in siltstones show different orientations and attitudes. Along W. Bali, foliations are striking N10°E and dipping 30° SE while along W. Mayyit Al-Abd, foliation strike is N60°E and dipping 20° toward SE. Fissility in siltstone and mudstone is strong turned to make penetrative foliation (Fig. 3b).

The investigated area is subjected to many tectonic events causing structural features, mainly represented by faults and joints. El Sirafe and Rabie (1989) reported five significant tectonic trends affecting G. Gattar namely NE-SW, NNE-SSW, N-S, NW-SE, and ENE-WSW.

Faults in the study area are mainly represented by strike slip type (dextral or sinistral) with some normal and reverse faults. The fault trends based on the total number proportion are arranged from the most common to the least common as follow: NNE-SSW, NE-SW, NW-SE, NNW-SSE, ENE-WSW, N-S, WNW-ESE and E-W. Faults are passing through all the exposed rock types in the investigated area. The faulted rocks are strongly brecciated, sheared and stained by hematite, silica, epidote, kaolin, chlorite and manganese dendritic shapes.

Rose diagram is constructed to determine the distribution of the faults recorded in the study area. It is concluded that the NNE–SSW is the predominant trend in G. Gattar granite (W. Bali) area (Fig. 4a). The second order of abundance is the NE–SW then NNW–SSE, while the NE–SW is the predominant trend in G. Abu Harba granite of W. Umm Sidra area (Fig. 4b) followed by the second order of abundance ENE–WSW then N–S.

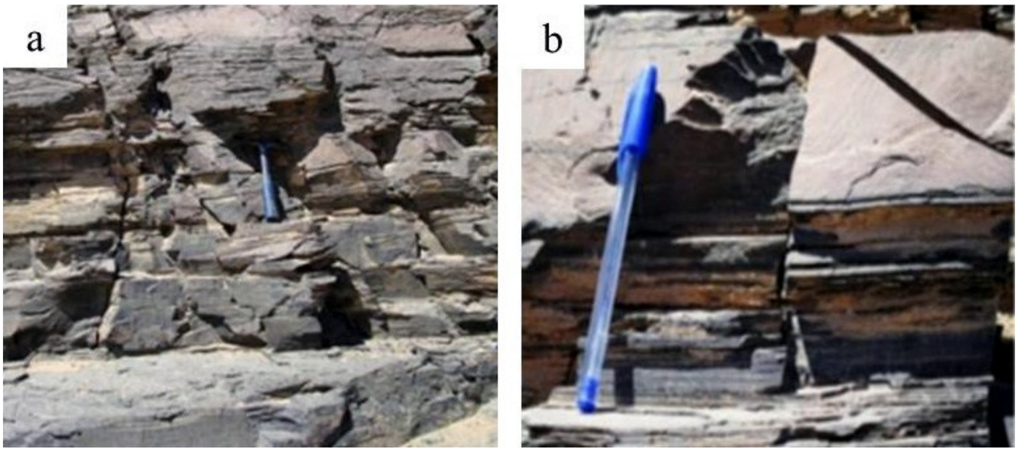

Fig. 3: (a) Closed view of bedding within the Hammamat sediments showing well-stratified siltstone beds, W. Bali, looking SE. (b) Well-developed fissility in the Hammamat siltstone, W. Umm Balad, looking N.

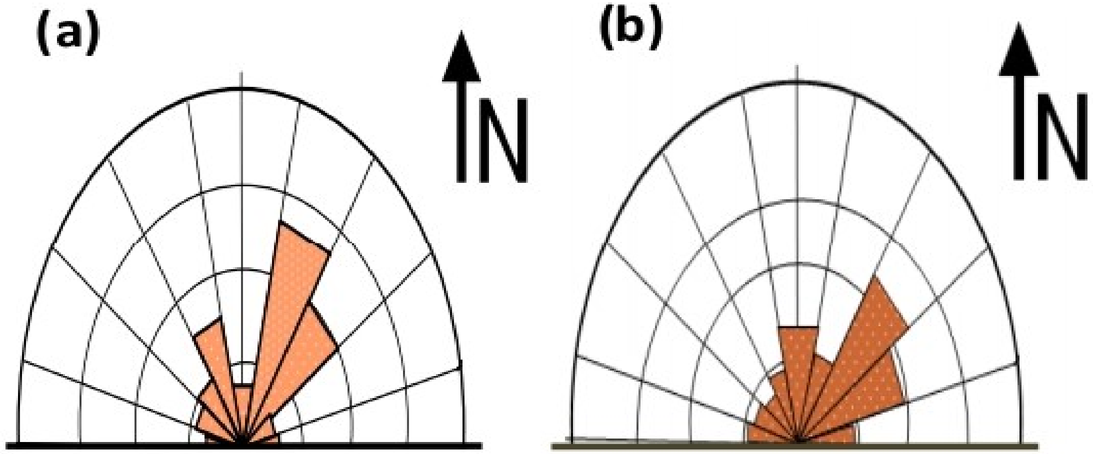

Fig. 4: (a) Rose diagram displaying the main directional fault trends measured in the Northern part of G. Gattar (W. Bali), (b) Rose diagram displaying the main directional trends faults measured in the southern part G. Abu Harba (W. Umm Sidrah).

The recorded faults in the study area can be belonging to two phases of compression stress (Fig. 5). The first phase is represented by compression force with maximum compression axis (σ) trends NNW-SSE forming two conjugate shear fractures which strike NNE-SSW with sinistral movements and WNW-ESE with dextral movement.

The second phase is represented by compression force with maximum compression axis (σ) which is rotated due to change in the tectonic events trending NE-SW in direction producing two conjugate shear fractures which strike NNE-SSW and ENE-WSW with dextral faults. The produced shear fractures of the second phase cause displacement and dislocation of shear fractures of the first phase thus they are younger than the shear fractures of the first phase. In the south of the study area, the same compression phases are occurred in G. Gattar batholith (Khamis, 1995).

The prevalent joint trends of the Dokhan volcanics is NNW-SSE trend followed by E-W and ENE-WSW trends (Fig. 6a). The main joint strike of Hammamat sedimentary rocks is N-S followed by NW-SE and NNW-SSE trends (Fig. 6b). In younger granites (G. Gattar), NE-SW joint strike is dominant followed by ENE-WSW strike (Fig. 6c). In younger granites (G.Abu Harba), NW-SE joint strike is dominant followed by E-W strike (Fig. 6d). Generally, the study area is affected by four main trends of joints represented by NNW-SSE, NE-SW, NW-SE and N-S trends.

Folding in the study area is represented by the major fold passing through W. Umm Balad. It is restricted to domain occupied by the Hammamat sedimentary rocks. Major folds in the Hammamat sediments are represented by only one broad anticlinal fold forming G. Um Tawat and are detected on both map scale and aerial photos (Fig. 7a). This major fold is located at the center of the structural map extending from NE to SW about 6 km long (Fig. 1). The northern limb shows a gentle dip reaching 25° to the NW at the contact with G. Dokhan. The southern limb is at the contacts with

G. Gattar with a steep dip reaching 75° SE. The change in the dip amount from the northern to the southern limbs indicates the asymmetrical character of this fold. Nearly horizontal beds dipping gently to the SW characterize the crest of the fold. The limbs of this fold show well-developed beds composed of alternation series of conglomerates, sandstones and siltstones.

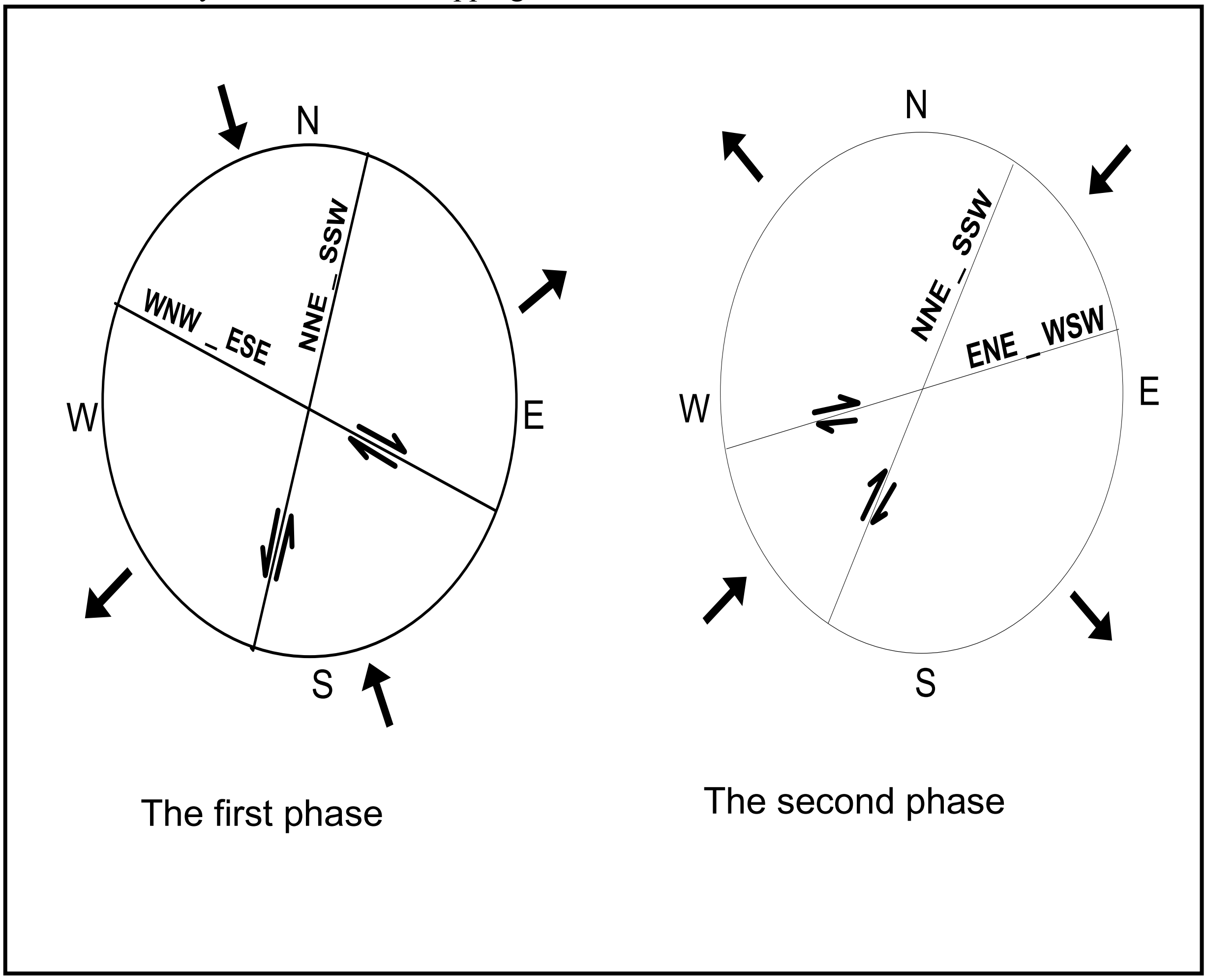

Fig. 5: Stress analysis of the major recorded faults in the study area.

(a)

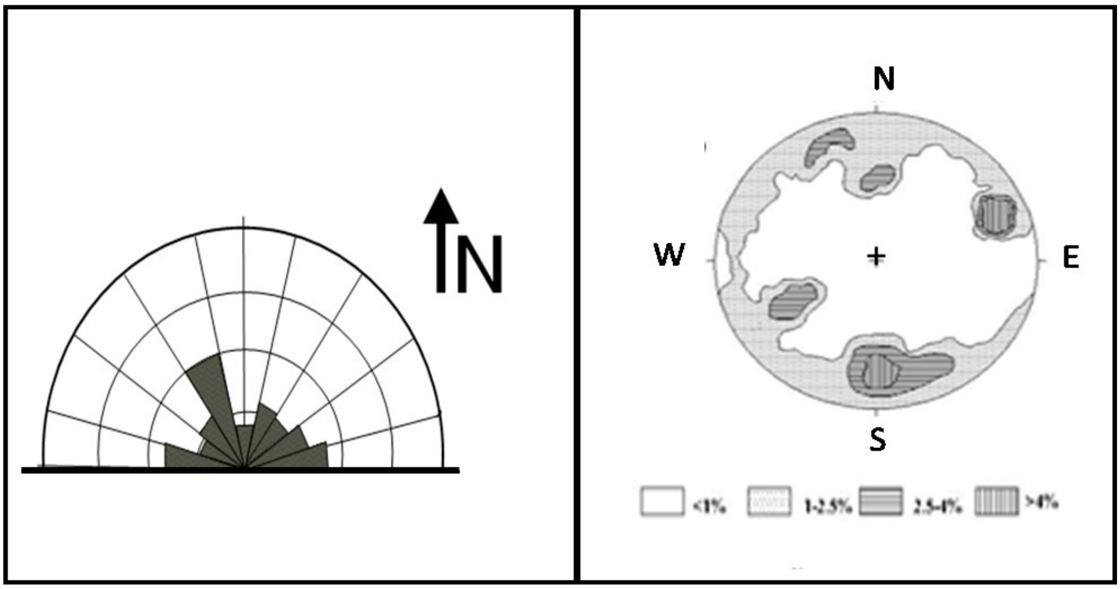

(b)

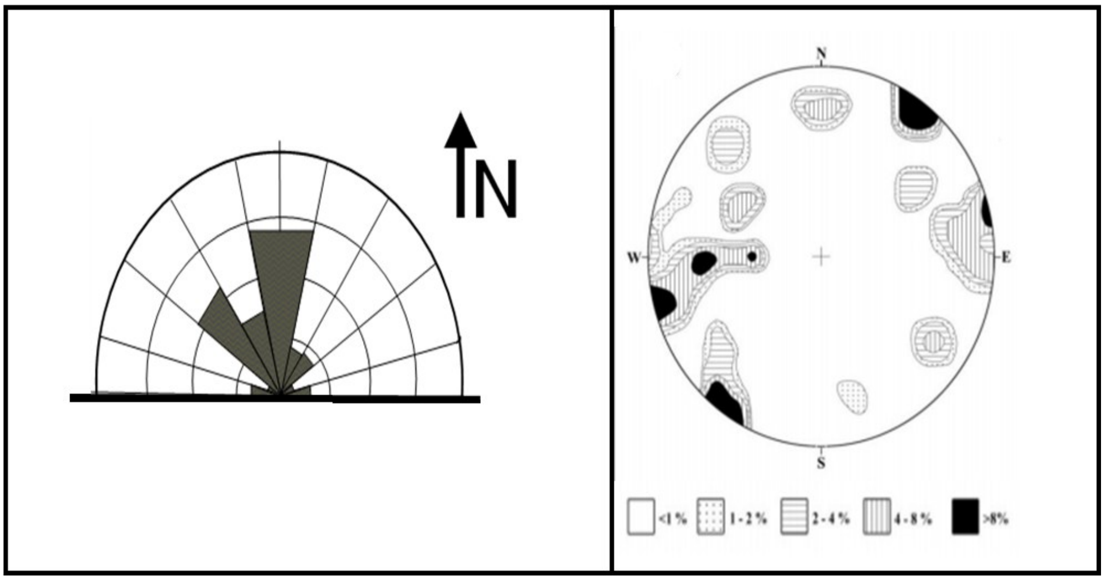

(c)

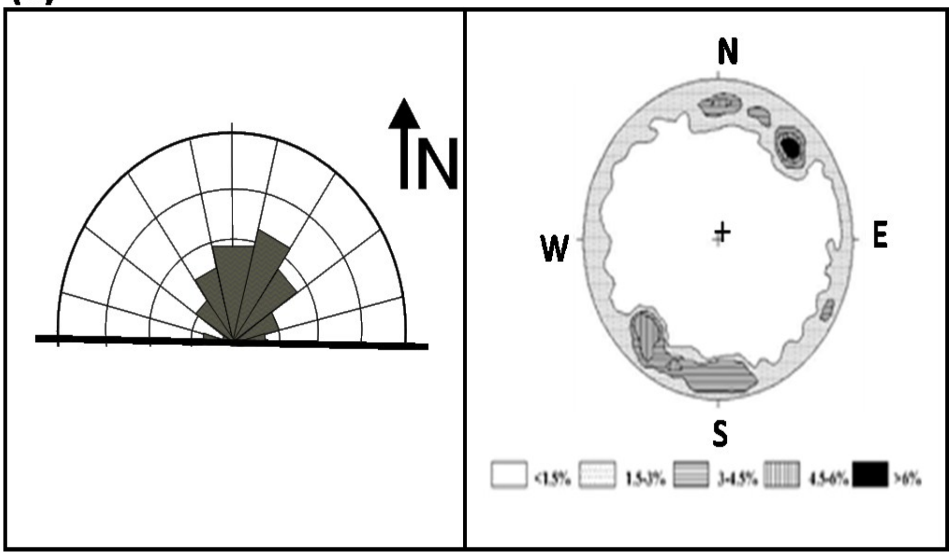

(d)

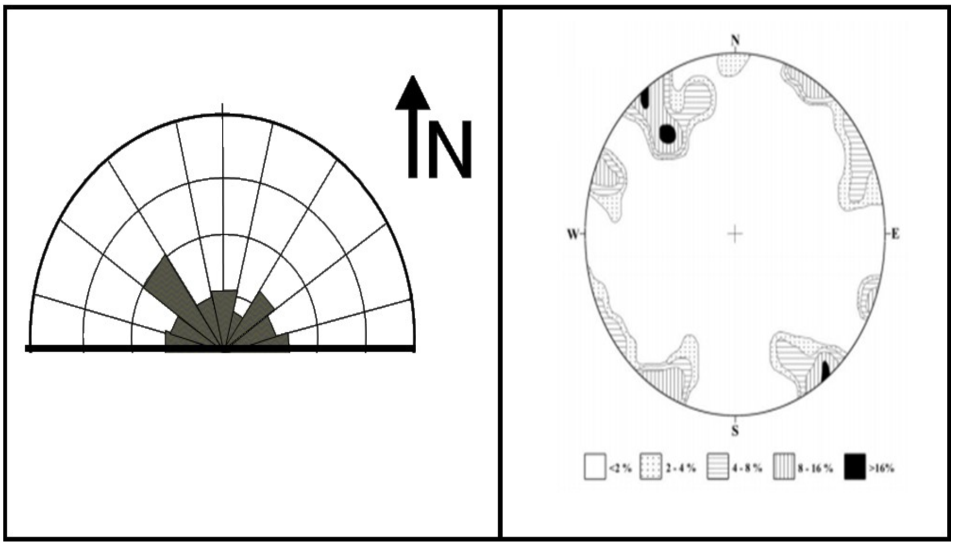

Fig. 6: Rose diagram and point contour diagram of joints in (a) Dokhan volcanics, (b) Hammamat sedimentary rocks, (c)younger granite rocks (G. Gattar), (d) younger granites (G. Abu Harba).

In the study area, the Hammamat sedimentary rocks were subjected to compression force trending NW-SE affected on the sedimentary rocks and because these rocks are ductile, they are folded forming major non plunging anticline fold (Fig. 7b). This fold is firstly formed with the beginning of compression and with increasing the amount of compression force, the rocks are fractured forming the faults which belong to the second phase.

This study is concentrated on the petrography of Gabal Gattar (alkalifeldspar granite and syanogranite) and Gabal Abu Harba (syanogranites).

Gabal Gattar alkali feldspare granites are very similar to the syenogranites where they are characterized by their high content of quartz and K-feldspar but they have low content of plagioclase relative to syenogranites. They are generally granular and composed of alkali-feldspar, quartz, plagioclase and biotite. Accessory minerals are zircon, monazite, xenotime and apatite, while muscovite and fluorite are minor minerals. Opaque minerals are magnetite, ilmenite and hematite.

K-feldspars are the most common minerals in these rocks. Potassic feldspars commonly consist of flamy and patchy perthitic crosshatched orthoclase with minor microcline. It occurs as subhedral to anhedral, coarse to medium-grained of plume, string, flame, feather and patchy perthites. Orthoclase perthite is mainly of string (Fig. 8a).

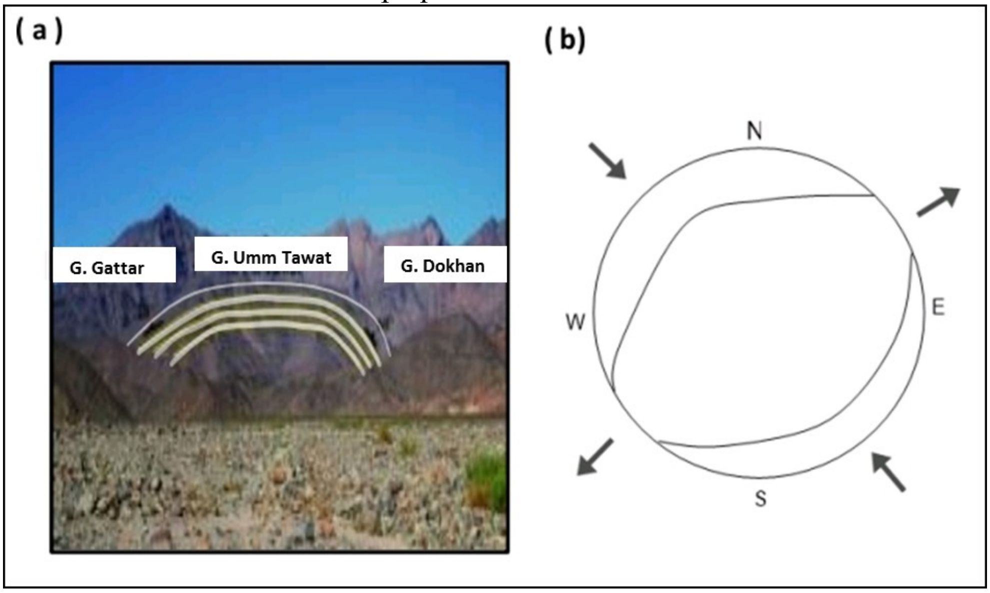

Fig. 7: (a) Major anticlinal fold forming G. Um Tawat Hammamat sediments W. Bali area, (b) A major non plunging fold recorded in Hammamat sedimentary rocks.

Quartz occurs as undulatory, anhedral to subhedral grains. Some crystals engulfed the orthoclase perthite (Fig. 8b). The quartz grains include muscovite, zircon and perthite as inclusions (Fig. 8c). Coarse-grained crystals of quartz corred the adjacent perthite resembling snowball structures (Fig. 8d).

Zircon occurs as short minute prismatic and highly metamict crystals in the quartz. Zircon is frequently present in clusters associated with iron oxides in distinct varieties of the Gattar granite.

Muscovite associated with quartz (Fig. 8e) and replaces biotite in all types of granite, but it is more abundant in alkali feldspar granites (Fig. 8f).

Microscopically, Gabal Gattar syanogranites are perthitic leucogranites essentially composed of perthites, quartz, plagioclase. Zircon, monazite, xenotime are the main accessory minerals. Muscovite, fluorite, biotite, and iron oxides represent the minor minerals. This granite type is coarse to medium grained and pinkish white, light pink to grayish pink in color. K-feldspars are the most common minerals in these rocks represented by orthoclase perthite and microcline perthite but the orthoclase perthites are the dominant. The perthite occurs as subhedral to anhedral, coarse to medium-grained of plume, string, flame, feather and patchy perthites (Fig. 9a). Orthoclase perthite is subhedral crystals showing simple twinning perthitic texture (Fig. 9b). Zircon is the most abundant accessory minerals in Gattar granite. It occurs as euhedral short prismatic crystals with brown, yellow tint. Zircon in most cases is rimmed with iron oxides (Figs.9c). Fluorite occurs as fine to medium-grained anhedral crystals with angular faces. It appears cleaved, cracked, isotropic and associated with iron oxides. Sometimes fluorite encloses quartz and zircon (Fig. 9d). It is colorless, pale rose and violet.

A systematic radiometric survey has been carried out on the various rock types exposed in the study area using a hand held scintillometer (model RS-230).

Dokhan volcanics display different levels and wide range of field gamma radioactivity due to ranging in their composition from intermediate (60-200 cps) to acidic (70-260 cps) with average 145.2 cps. They have eU concentrations range from 2.0 to 6.0 ppm with an average of about 4.0 ppm. The eTh varies from 6.0 to 17.0 ppm with about 11.5 ppm in average.

Hammamat sedimentary rocks display different variation due to variations in lithology. The total gamma radioactivity ranges from 160 to 220 cps. The gamma radioactivity of Hammamat sedimentary rocks increases at their contacts with the younger granites. They have eU concentrations reach 6.0 ppm with an average of 3.0 ppm and sometimes show ULD of eU contents. The eTh varies from 5.0 to 17.0 ppm with about 11.0 ppm in average.

Radiometric studies revealed that radioactivity of younger granites is higher than that of Dokhan volcanics and Hammamat sedimentary rocks due to: (a) the mineralogical composition, (b) degree of acidity, (c) amount of the accessory minerals such as zircon, monazite, apatite, sphene and iron oxides which capture radioactive elements (U and/or Th) within their crystal lattices, (d) Structural features controlling by alteration where the younger granites along these structures are strongly hematitized and silicified. The hematite is characterized by adsorbing uranium from the circulating solutions and (e) presence of pegmatites and silica veins which entrap uranium in their composition. Also hydrothermal activity plays an important role in increasing the uranium content in younger granites where it remobilizes fixed U into fluid phase then transports it to favorable places where ore precipitation is then accompanied by intense alteration processes (Zhang et al., 2006).

Uranium mineralization in the host rocks occurs as pitchblende (primary uranium mineral) and as uranophane; beta-uranophane (secondary origin) and they are strictly fault-bounded as they are strongly linked to the fault activities (Waheeb, 2021).

Uranium mineralization along northern part of Gabal Gattar (W. Bali) area.

1) <u>(GIII) Uranium Occurrence in north Gabal Gattar:</u>

This occurrence is situated at the northern parts of Gabal Gattar along a NNE-SSW trending shear zone steeply dipping between 60° and 70° to the ESE direction (Fig. 1). It is extending about 2 km in length and varies in width from lm to more than 10 m.

The occurrence of uranium mineralizations of GIII occurrence are associated with alterations represented by the hematitization, silicification and kaolinitization. Uranium mineralizations are occur as lenses at the intersection of the cross-joints and fractures (Fig. 10).

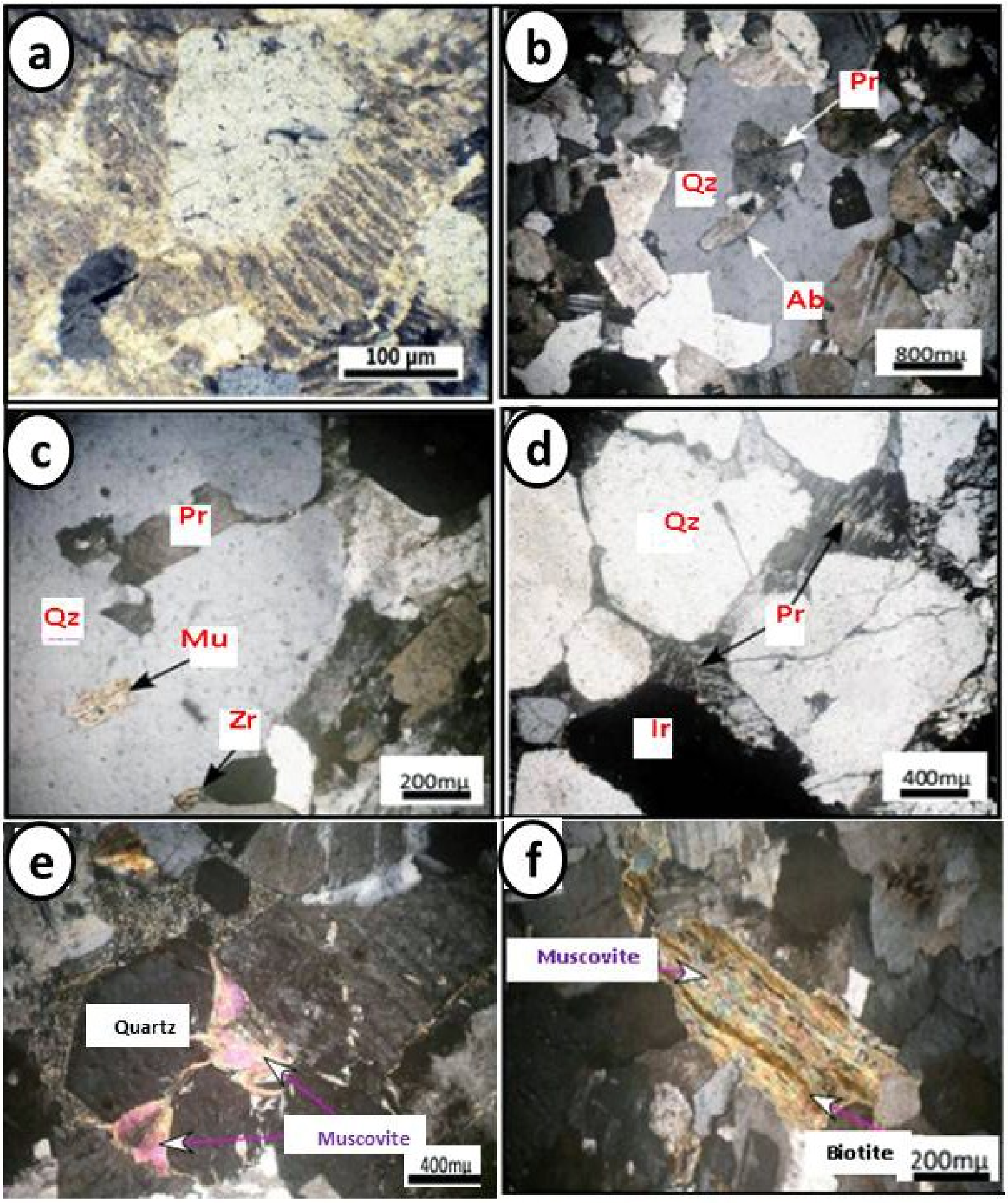

Fig. 8: Photomicrographs display a) String perthite in Gattar alkali feldspar granites, C.N. b) Anhedral crystal of quartz containing laths of albite and perthite, C.N. c) Perthite engulfed in quartz C.N. d) Rounded coarse-grained quartz (resembling snowball texture), C.N. e) Fan-shaped muscovite associated with quartz, C.N. f) Muscovite commuting biotite, C.N.

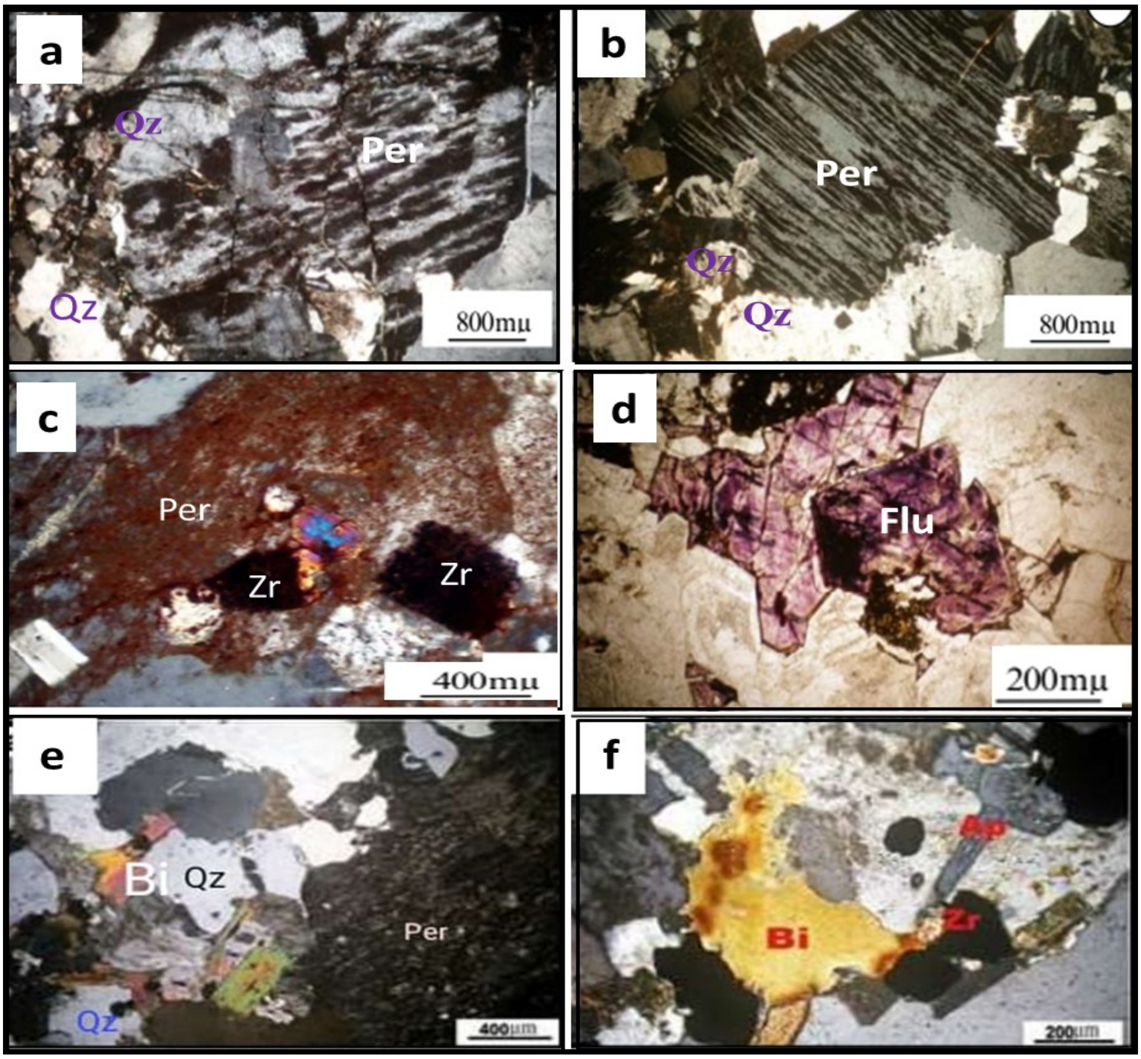

Fig. 9: Photomicrographs display (a) Flame perthite surrounded by quartz in G. Gattar syenogranite, C.N., (b) Subhedral crystal of perthite corroded by quartz in G. Gattar syenogranite, C.N., (c) Violet fluorite associated with quartz in G. Gattar syenogranite, P.L., (d) Zoned zircon included in perthites stained with iron oxides in G. Gattar syenogranite, C.N., (e) Phenocrystal of perthite, quartz and biotite in G. Abu Harba syenogranite, C.N., (f) Minute crystal of zircon associates biotite and apatite G. Abu Harba syenogranite, C.N.

One selected sample of high uranium mineralization has been radiometrically analyzed. This sample is taken from GIII occurrence; where it recordes eU 2650 ppm, while eTh content is 75 ppm and the average eTh/eU ratio is 0.028 (Table.1).

2) <u>(GII) Uranium Occurrence in north Gabal Gattar):</u>

GII Uranium Occurrence is located along a shear zone parallel to Gl shear zone, striking N12°E to N25°E and dipping 60° to 70° ESE (Fig. 1). The granite in this occurrence is brownish red in color.

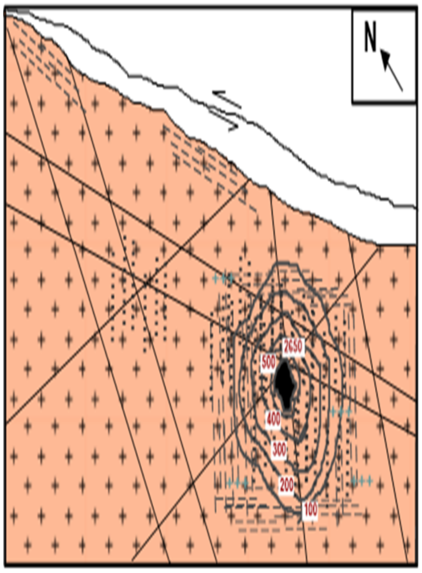

Table 1: eU and eTh contents in (ppm) **of GIII Granite occurrence.**

Sample	eU (ppm)	eTh (ppm)	**eTh/eU**
1	2650	75	**0.028**

Fig. 10. Geological and alteration map of uranium occurrence GIII.
(lat. 27º 06' 43" N long. 33º 16' 15" E)

Along this shear zone the secondary uranium mineralizations are recorded and is controlled by fractures and joints. The richest uranium ore bodies are distributed along a nearly E–W striking shear zone that transected by mineralized NS, NNE to NE and NW trending fractures (Abdel Hamid et al, 2023). They are usually associated with most common alteration features as hematitization, silicification and fluoritization and associated with other alterations as manganese dendrites, albitization, limonite and kaolinite (Fig. 11). Fluorite varying from violet to dark violet or black is recorded in the uranium mineralized zones.

Geological and radiometrical studies of the G-II uranium occurrence revealed the presence of many secondary uranium mineralizations and also primary uranium minerals. Uranium mineralization is distributed in the form of veins or coating on joint surfaces and fissures. The intensity of mineralization greatly increases at the intersection zones of fractures and faults.

Some selected uranium mineralized samples have been radiometrically analyzed. The eU ranges from 59 to 4810 ppm with an average 1271 ppm while eTh contents range from 13 to 270 ppm with average 64ppm. The average eTh/eU ratio is around 0.104 reflecting high enrichment of uranium mineralizations (Table. 2).

3) <u>(GV) Uranium Occurrence in north Gabal Gattar:</u>

W. Bali uranium occurrence (G-V uranium occurrence) can be considered as a possible potential deposit for uranium (U), rare earth elements (REE) + Y (yttrium), and other rare metals, as well as the mineralization, are caused by alkaline and oxidizing hot fluids, with the contribution of meteoric water volume heated by convection (Waheeb, 2022 b).

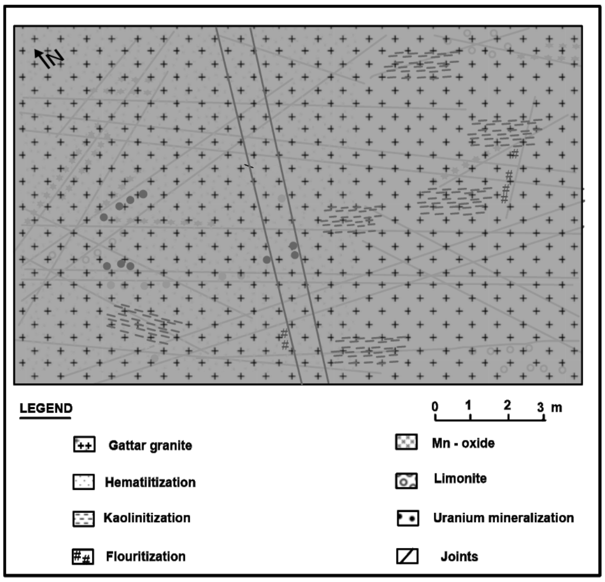

Fig.11. Geological map and uranium occurrence of GII granite.
(lat. 27º 06ʹ 26ʺ N long. 33º 16ʹ 35ʺ E)

Table 2: eU and eTh contents in (ppm) of GII Granite occurrence.

Sample	eU (ppm)	eTh (ppm)	eTh/eU
1	59	23	0.39
2	570	20	0.035
3	148	31	0.2
4	1230	50	0.04
5	420	30	0.07
6	2710	100	0.036
7	220	25	0.113
8	3300	270	0.08
9	4810	150	0.03
10	330	35	0.106
11	135	20	0.14
12	1320	13	0.009
Average	1271	64	0.104

This uranium occurrence lies at the contact between the Hammamat sediments with Gabal Gattar granite at the southern bank of Wadi Bali. It is controlled by a local reverse fault trending ENE-WSW along the contact between the granites and the sediments.

The uranium mineralization is mainly confined to the Hammamat sediments rather than the episyenitized granites. The secondary uranium mineralization is of intermittent nature and occurs as lensoidal bodies. Uranium mineralization is confined to the NE-SW, ENE-WSW, NW-SE and NNE-SSW trends. The main alteration features associating the secondary uranium mineralized zones in both sides of G-V uranium occurrence, include hematitization, bleaching, episyentization, kaolinitization, fluoritization and silicification.

Some selected mineralized samples are measured radiometrically where the eU ranges from 15 to 2740 ppm with an average 588ppm, while Th contents ranges from 12 to 470 ppm with an average 90 ppm. The average eTh/eU ratio is around 0.72 reflecting the high enrichment of uranium mineralization (Table. 3).

The high density of uranium mineralization is concentrated at the eastern and westem side of the contact of G-V uranium occurrence associated with highly silicified and hematitized parts of the granite (Fig. 12).

Uranium mineralization along the southern part of Gabal Abu Harba (W. Umm Sidra) area.

The uranium mineralization in G. Abu Harba alkali feldspar granite are located along sheared, silicified and altered regions at its western marginal parts (Fig. 13). Secondary uranium minerals occur as patches or fill microfractures. Some other radioactive anomalies have been detected through this granite near places of uranium mineralization.

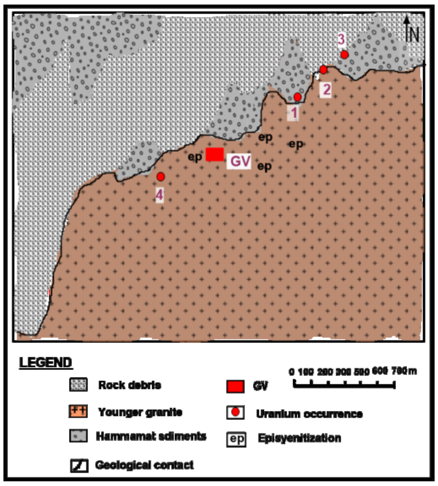

Fig.12. Geological map and uranium occurrence of GV granite.
(lat. 27º 07' 15" N long. 33º 17' 28" E)

Table 3: eU and eTh contents in (ppm) of GV Granite occurrence.

Sample	eU (ppm)	eTh (ppm)	eTh/eU
1	15	23	1.5
2	25	30	1.2
3	18	24	1.33
4	2025	70	0.03
5	170	12	0.07
6	36	18	0.5
7	57	35	0.61
8	780	470	0.6
9	20	27	1.35
10	2740	200	0.072
Average	588.6	90	0.726

Radioactive anomaly was discovered on the western marginal parts of G. Abu Harba. At this location, the granite suffered from a strong mylonitization and jointing. The radioactive anomalies are generally limited to area of intersection of N-S and NE-SW trending fractures (Fig. 14a). The main alteration features around these spots are strong hematitization and kaolinitization. The uranium concentration through the radioactive anomaly is ranging from 100 to 350 ppm with average of 220 ppm (Fig. 14b). The distribution of uranium mineralization is structurally and lithologicaly controlled; along W. Umm Sidra.

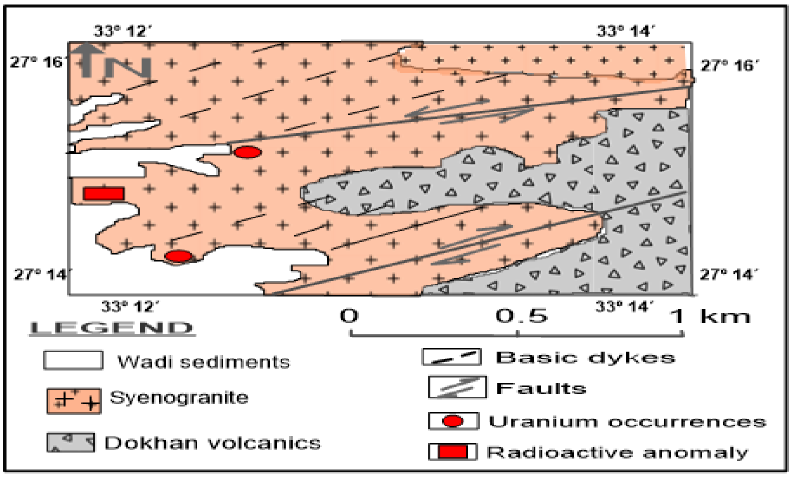

Fig. 13: Geological sketch map of structurally controlled Uranium mineralization lithological controlled radioactive anomalies in G. Abu Harba (west W. Umm Sidrah) area.

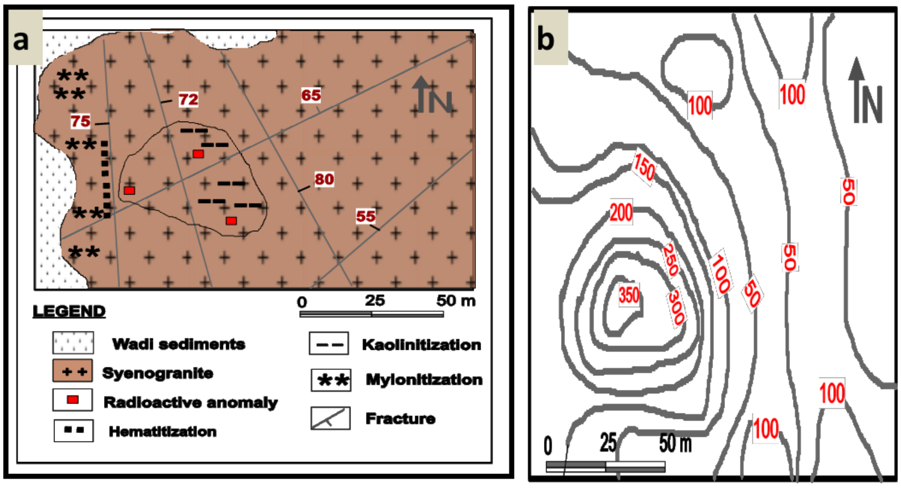

Fig. 14: (a) Geological sketch and (b) Isorad map of the radioactive anomaly.

CONCLUSIONS

The study area is located in the northern part of the Eastern Desert of Egypt. It is situated in the northern sector of the Red Sea mountain ridges at about 65 km northwest of Hurghada City. It includes Neoproterozoic basement rocks comprising Dokhan volcanics (oldest), Hammamat sedimentary rocks, younger granites and post granite dykes (youngest).

The younger granites are distinguished into G.Gattar granites and G. Abu Harba granites. G. Gattar granites are composed of perthitic leucogranites essentially composed of a nearly equal amount of perthites, quartz, plagioclase. Zircon, monazite, xenotime are the main accessory minerals. Muscovite, fluorite, biotite, calcite and iron oxides (opaque minerals) represent the minor minerals.

G. Abu Harba granites are characterized by equigranular texture between quartz, perthites, plagioclase and biotite. Zircon, apatite, fluorite, muscovite and iron oxides are the main accessory minerals. Epidote and chlorite represent the secondary minerals.

The study area is mainly affected by faults and joints of different trends. The abundant fault sets are NNE-SSW, NE-SW, NW-SE and N-S and all faults are of compression stress. Faults are passing through all the exposed rock types and wadis in the investigated area. The faulted rocks are strongly brecciated, dissected and stained by hematite, silica, epidote, kaolin, chlorite and manganese dendritic shapes. Four main trends of joints cutting the area with NNW-SSE, NE-SW, NW-SE and N-S trends and all joints in the area are of tension stress.

Radioactivity of younger granites is higher than that of the other older rocks. Radioactive anomaly is recorded in western marginal parts of G. Abu Harba granites. The granite suffered from a strong mylonitization and jointing. It is controlled by lithology containing U and Th-bearing minerals of uranophane, thorite and zircon in addition to alteration features around these spots represented by hematitization, kaolinitization and iron oxides which capture U and/or Th elements.

Along GII occurrence the eU ranges from 59 to 4810 ppm with average 1271 ppm, while Th contents ranges from 13 to 270 ppm with an average 64ppm.

At GV occurrence the eU ranges from 15 to 2740 ppm with an average 588, while Th contents range from 12 to 470 ppm with an average 90 ppm.

The younger granites in the study area have (a) high background levels of U and Th, (b) hydrothermal alterations in many places, (c) metamictized radioactive minerals as zircon, (d) many bodies of pegmatites, aplite and quartz veins and (e) controlled structural features of joints, strike slip faults and dykes. These factors represent a favorable environment for secondary uranium generation, so we recommend more detailed radiometric survey for the area where more radioactive anomalies are expected, especially in Gabal Abu Harba.

REFERENCES

Abdel Hamid, A.A., 2013. Mineralogical and geochemical studies of the uranium-bearing granites, Gabal Abu Harba area, North Eastern Desert, Egypt. Ph. D. Thesis, Fac. Sci., Benha Univ., Egypt, 173P.

Abdel Hamid, A.A., Abdel Hamid, H.M., Seddik S.H., and Metwally, M.M., 2023. Mineralization Styles and Alteration Paragenesis of Metasomatic Zones in the Highly Fractionated Granite of Gabal Gattar, Northern Eastern Desert, Egypt. Middle East Journal of Applied Sciences. V. 13. Issue. 3. P. 441-457.

Abu Zaid, M.M., 1995. Relation between surface and sulsurface uranium mineralization and structural features, Gebel Gattar, North Eastern Desert, Egypt: M. Sc. Thesis, Fac. Sc, Ain Shams Univ., Cairo, Egypt, 208 P.

Dardir A.A., Abu Zeid K.M., 1972. Geology of the basement rocks between latitudes 27° 00′ and 27° 30′ N, Eastern Desert. Ann Geol Surv Egypt 2:129–158.

El-Sirafe, A.M. & Rabie, S.J., 1989. Contribution of aeromagnctic to structural mapping of Gabal Gattar area, north Eastern Desert, Egypt-Jour, afric. Earth Sci., 10/3: 132-155.

Hamimi, Z., Abd El-Wahed, M.A., Gahlan, H.A., and Kamh, S.Z., 2019. Tectonics of the Eastern Desert of Egypt: key to understanding the Neoproterozoic evolution of the Arabian-Nubian Shield (East African Orogen). In: A. Bendaoud et al. (eds.), The Geology of the Arab World-An Overview. Springer Nature, Switzerland, 1-81.

Khamis, H.A., 1995. Radioactivity and structure of Wadi Hammad area, North Eastern Desert, Egypt. M. Sc. Thesis, Fac. Sci., Cairo Univ., Egypt, 235 P.

Roz, M.E., 1994. Geology and uranium mineralization of Gabal Gattar area, North Eastern Desert, Egypt. M. Sc. Thesis, Fac. Sci., Al Azhar Univ., Egypt, 175 P.

Roz, M.E., 2001. Geology and uranium potentialities in Gabal Abu Harba environs, North Eastern Desert, Egypt. Ph. D. Thesis, Fac. Sci., Cairo Univ., Egypt, 264 P.

Salman, A.B., El Assy, I.E. and Shalaby, M.H., 1990. New occurrence of uranium mineralization in Gebel Gattar, northern Eastern Desert. Egypt: Ann. Geol. Surv. Egypt. V. XVI, P. 31 - 34.

Shalaby, M.H., 1990. Uranium mineralization in northern Gebel Gattar locality, northern Eastern Desert: 7 th Conf. Phanerozoic and Develop. Al Azhar Univ. Cairo, (In pressShalaby, M.H., 1996: Structural controls of uranium mineralization at Gabal Qattar, north Eastern Desert, Egypt: The Egyptian Academy of sciences Proceedings, (In press).

Stern, R. J., 1985. The Najd fault system, Saudi Arabia and Egypt: a Late Precambrian rift-related transform system. Tectonics, 4, 497-511.

Stem, R.J. & Hedge, C.E., 1985. Geochronologic and isotopic constraints on Late Precambrian crustal evolution in the Eastern Desert of Egypt - Amer. Jour. Sci., 285: 97-127.

Waheeb, A.G., and El Sundoly, H.I., 2016. Structure roles for the localization of metasomatite uranium deposit type at Wadi Belih area, Northern Eastern Desert, Egypt. Egypt. J. Geol., 52, 201-214.

Waheeb, A.G., 2017. Detailed structural analysis for the mineralized shear zones of G-II uranium occurrence at Gabal Gattar younger granite Northern Eastern Desert Egypt. Int. J. Innov. in Eng. and Tech. (IJIET), ISSN, 2319-1058.

Waheeb, A.G., 2021. Resolved Shear For the Uranium Mineralized Fault Contacts at Gabal Abu Hamr and Gabal Gattar, Northern Eastern Desert, Egypt. Annals of Geol. Surv. Egypt. V. XXX VIII , P. 243 -255.

Waheeb, A.G., and Samaan, J.M., 2021. Comparison between the Structurally Controlled Radioactive Min¬erals at Felsic Granites of G. Abu Harba, G. Dara and G. Hamrat Al Jirjab Areas, Northern Eastern Desert, Egypt. Egyptian Journal of Geology. V. 65, P.1-12

Waheeb, A.G., 2022a. Structural Pattern Controlling the Localization of Radioactive Mineralizations at Gabal Gattar and Wadi Ras Abda Areas , Northern Eastern Desert, Egypt. International Journal of Latest Trend in Engineering and Technology (IJLTET).V.21. Issue 1 . P. 6-15.

Waheeb, A.G., 2022b. Tension Gashes Explore the Structural Deformation of Mineralized Shear Zone at Wadi Belih, Northern Eastern Desert, Egypt. The Bulletin of Tabbin Institute for Metallurgical Studies (TIMS). V.110. P. 42-55.

الخصائص الصخرية والتركيبية المتحكمة في التمعدنات المشعة في الصخور الجرانيتية الحديثة بمنطقة وادي بلي ووادي ام سدرة، شمال الصحراء الشرقية، مصر

عبداللة سعد عبدالنبي[٢] واحمد محمد المزين[١] و درويش محمد الخولي[٢] و حسام انور خميس[٢]

٢ هيئة المواد النووية – القاهرة – المعادى – مصر. ١ قسم الجيولوجيا – كلية العلوم – جامعة الازهر

الخلاصة

تقع منطقة الدراسة شمال الصحراء الشرقية المصرية بين خطي عرض ″35 ′06 °27و °27 ″40 ′15شمالا وخطي طول ″18 ′00 °33 و″25 ′10 °33 شرقاً. وتُغطّي بصخور البروتيروزوي

الحديث والتي أمكن تقسيمها وترتيبها إعتماداً علي الدراسات الحقلية إلى بركانيات جبل الدخان (الأقدم) ومجموعة صخور رسوبيات الحمامات والجرانيت الحديث وقواطع ما بعد الجرانيت (الأحدث).

يمثل الجرانيت الحديث الوحدة الصخرية الأساسية في المنطقة حيث أنه الأوسع انتشاراً في المنطقة كلها. وتتمثل في جرانيت جبل جتار وجرانيتات جبل ابو حربة.

ولقد تأثرت منطقة الدراسة بإتجاهات رئيسية من الفواصل هي كالاتي: في الجرانيتات الحديثة لجبل جتار الإتجاهات السائدة للفواصل هي شمال شرق – جنوب غرب هي السائدة تليها هو شرق شمال شرق – غرب جنوب غرب بينما في الجرانيتات الحديثة لجبل ابو حربة الإتجاهات السائدة للفواصل هي شمال غرب – جنوب شرق يليها بواسطة اتجاة شرق – غرب.

وأظهر المسح الإشعاعي للمنطقة أن قيم الإشعاعية للجرانيت الحديث أعلي من مثيلتها للصخور الأخري الأقدم وترجع هذه القيم العالية للجرانيت إلي التركيب المعدني ودرجة الحامضية وكمية المعادن الثانوية الموجودة به مثل معادن الزيركون والمونازيت والأباتيت والإسفين وأكاسيد الحديد وأيضاً ترجع إلى تأثير التراكيب الجيولوجية والتي تعمل علي حجز المعادن المشعة كما ترجع إلى وجود عروق المرو والبجماتيت الحاملة لليورانيوم والثوريوم. وسجلت الشاذة الإشعاعية في البجماتيت النطاقي في صخور الجرانيت الحديث من الجزء الشمالي الغربي لجبل ابو حربة.

وقد وجد أن الجرانيت الحديث في المنطقة يمتلك محتوي عالي من اليورانيوم والثوريم والتغيرات المصاحبة للمحاليل الحارة والعديد من البجماتايت وعروق الكوارتز والأبليت وكذلك العديد من التراكيب الجيولوجية من الفواصل والصدوع والقواطع. كل هذا يشير إلي بيئة مناسبة لتكون معادن اليورانيوم الثانوية لذا نوصي بإجراء مسح إشعاعي أكثر تفصيلا حيث من المتوقع إستكشاف المزيد من الشاذات الإشعاعية خاصة في جبل ابو حربة.